NON-CONTACTING TECHNIQUES FOR PLANT DROUGHT STRESS DETECTION

Y. Yang, P. Ling, D. H. Fleisher, D. J. Timlin, V. R. Reddy

ABSTRACT. *Plant drought stress indicators such as crop water stress index (CWSI), plant motion in the form of covariance of top-projected canopy area (COV_{TPCA}), leaf water content represented as equivalent water thickness (EWT), and their threshold values for drought stress detection were established from measurements. Performances of these indicators in detecting drought stress of New Guinea Impatiens plants in a controlled environment were evaluated. Analysis of variance (ANOVA) was conducted to compare the timing of drought stress detection by these indicators against the timing of incipient drought stress defined by evapotranspiration (ET) and timing of human visual detection. Statistical analysis was also performed to study the consistency of the threshold values of the indicators in different experiments. ANOVA results showed that the CWSI was the most reliable indicator for early plant drought stress detection. The timing of the drought stress detection from the earliest to the latest was CWSI, EWT, and COV_{TPCA}. While COV_{TPCA} and EWT were not able to detect drought stress as early as CWSI, ANOVA results indicated that these two indicators were able to detect drought stress no later than visual detection. ANOVA results also showed that there was no significant difference in threshold values of CWSI and COV_{TPCA} in different experiments, but different cultivars used in the experiments resulted in significant differences in EWT threshold values.*

Keywords. *Controlled-environment agriculture, Crop water stress index (CWSI), Equivalent water thickness (EWT), Irrigation scheduling, Plant monitoring, Top-projected canopy area (TPCA).*

Plant drought stress refers to the condition in which plant cells and tissues are at less than full turgor. This occurs whenever the loss of water by transpiration exceeds the rate of water absorption (Kramer, 1969). With the occurrence of drought stress, almost all of the processes associated with plant growth are affected. Severe drought stress affects the accumulation of biomass, limits plant productivity and yield by reducing photosynthesis and leaf growth, and affects partition of biomass to the harvestable parts of the plant (Hsiao, 1981; Boyer, 1982; Bradford and Hsiao, 1982; Saini and Lalonde, 1998).

Substantial increases in yield could be possible if irrigation water was applied at the most appropriate time to prevent excessive drought stress. With the increase in the cost of energy required to pump and move water to desired locations, coupled with the decrease of available water for irrigation, it is essential to attain the maximum benefit from each unit quantity of water used for irrigation. Plant drought stress detection is thus of great importance.

Human visual assessment of crop stress is qualitative at best, with the terms "good" or "poor" frequently used to describe crop condition (Jackson et al., 1986). To improve the monitoring and irrigation process, automatic monitoring and quantitative describing of plant water status are necessary.

Sensors for plant water content measurements are available commercially. Examples include the pressure bomb (Scholander et al., 1965; Longenecker and Lyerly, 1969) and the leaf diffusion porometer (Kanemasu et al., 1978). These methods are intrusive to plants, and the measurement procedure is time consuming. Therefore, characterizing drought stress using these methods is not practical for mass plant production. A non-contacting, non-intrusive sensing technique based on direct measurement of plant condition is desirable for *in situ* plant water status monitoring.

Plant leaf surface temperature has long been related with plant drought stress (Ehrler et al., 1978a, 1978b). Infrared thermocouple temperature sensors have made non-contacting measurement of plant leaf surface temperature possible. Jackson et al. (1981) and Idso et al. (1981) developed the crop water stress index (CWSI) from the measurement of the canopy temperature and the vapor pressure deficit (VPD) of the air. The calculation of CWSI is based on the balance of total energy, consisting of sensible heat, which heats the plant, and latent heat, which is used for transpiration. The assumption is that when a plant is transpiring at its full potential rate, the leaf temperature is supposed to be 1° C to 4° C below the air temperature, and the CWSI has a value of 0. When a plant is experiencing drought stress, the transpiration rate decreases, and the leaf surface

Submitted for review in December 2007 as manuscript number IET 7325; approved for publication by the Information & Electrical Technologies Division of ASABE in July 2008.

The authors are **Yang Yang, ASABE Member,** Research Associate/Visiting Scientist, USDA-ARS Crop System and Global Change Laboratory, Wye Research and Education Center, University of Maryland, Beltsville, Maryland; **Peter Ling, ASABE Member,** Associate Professor, Department of Food, Agricultural and Biological Engineering, The Ohio State University, Wooster, Ohio; and **David H. Fleisher, ASABE Member Engineer,** Agricultural Engineer, **Dennis J. Timlin,** Soil Scientist, and **Vangimalla R. Reddy,** Plant Physiologist, USDA-ARS Crop Systems and Global Change Laboratory, Beltsville, Maryland. **Corresponding author:** Yang Yang, USDA-ARS Crop System and Global Change Laboratory, Wye Research and Education Center, University of Maryland, 10300 Baltimore Ave., Bldg. 1, Room 201, Beltsville, MD 20705; phone: 301-524-5269; fax: 301-504-5823; e-mail: yang.yang@ars.usda.gov.

 © 2008 American Society of Agricultural and Biological Engineers ISSN 0001−2351

temperature gradually becomes higher than the air temperature, resulting in a higher CWSI value. The CWSI value becomes 1 when the plant is no longer transpiring.

CWSI has been widely applied to study the effect of drought stress on plant yield and quality (Halim et al., 1990; Garrot et al., 1993; Irmak et al., 2000; Moller et al., 2007), to determine the water requirement of plants (Samis and Jernigan, 1992; Fereres et al., 2003; Goldhamer, 2005; Wang et al., 2005), and to schedule irrigation (Garrot et al., 1997; Yazar et al., 1999; Naor et al., 2006; Testi et al., 2008). Kacira and Ling (2001) and Kacira et al. (2002a) studied the feasibility of using CWSI to detect plant drought stress in a controlled environment. The research found that the established CWSI threshold value was able to detect drought stress in New Guinea Impatiens plants one to two days prior to visual detection of the stress symptom.

Leaf motion is driven by variation in the turgor potential of the pulvinus (or pulvinule) organ at the base of the leaf blade. In addition to normal diurnal movement, plant leaves also move in response to biotic/abiotic stresses. Nyakwende et al. (1996) correlated the boundary movement of plants with drought stress. Naor (2006) and Moller et al. (2007) reported their efforts in applying visible band imageries to estimate plant water status. Kacira et al. (2002b) computed the top-projected canopy area (TPCA) and its coefficient of variation (COV_{TPCA}) for well-watered and drought stressed New Guinea Impatiens plants and demonstrated that the value of COV_{TPCA} could indicate the occurrence of drought stress 5 to 29 h before the onset of visual wilt symptoms.

Jacquemoud (1993) developed a multispectral reflectance model named PROSPECT+SAIL to simulate plant canopy reflectance as a function of leaf biochemistry, canopy architecture, and observing geometries. In the PROSPECT+SAIL model, water in the leaf is assumed to be a single layer of water averaged over the entire leaf, and water content in the leaf is quantified by equivalent water thickness (EWT). A brief introduction to the models is provided in the Appendix. Jacquemoud et al. (1995) inverted the PROSPECT+SAIL model using a set of 96 airborne visible/infrared imaging spectrometer (AVIRIS) equivalent spectra gathered in a field experiment on sugar beet plots. The structural parameters of the canopy were poorly estimated. The PROSPECT+SAIL model estimated water content reasonably well: the root mean square error (RMSE) was between 0.128 to 0.234 mm, while the measured water depth was between 0.3 to 0.5 mm. Yang and Ling (2004) developed an inversion procedure of the PROSPECT+SAIL model to estimate the EWT of New Guinea Impatiens from measured canopy reflectance in a controlled environment. EWT is directly linked to the amount of water within plant leaves. Therefore, it might be a good indicator for plant drought stress. However, so far, the model inversion technique has not yet been applied in plant drought stress detection.

The goal of this study was to examine non-contacting techniques for plant drought stress detection. Efforts were centered on confirming the previous findings of the performance of CWSI and COV_{TPCA} in drought stress detection, and evaluating performances of these techniques in drought stress detection. The objectives of this study were to:

- Validate the effectiveness of using CWSI and COV_{TPCA} in drought stress detection.
- Evaluate the feasibility of using the retrieved EWT in the plant drought stress detection.
- Evaluate the performance of the three indicators in drought stress detection.

Materials and Methods

Data Collection

Five experiments were conducted in a walk-in growth chamber equipped with high-intensity discharge (HID) lamps (Yang and Ling, 2004). New Guinea Impatiens was used as a model plant in the experiments. In each of the five experiments, six pots of plants with similar appearances and sizes were used. Three of these plants were designated as treatment plants and the other three as control plants. Prior to each experiment, plants were transplanted into 152 mm pots and were watered thoroughly. After an experiment was started, the control group plants were kept well watered, while water was withheld from the treatment plants. In experiments 3 and 4, after the drought stress symptoms were visually observed, the treatment plants were irrigated again and subjected to a second cycle of drought stress treatment. As a reference, the duration of each experiment, the cultivar variety of plants used, and the environmental conditions in the growth chamber are listed in table 1.

The weight of each pot of plants was measured continuously with a custom-built lysimeter consisting of a load cell (model 355, Tedea-Huntleigh, Chatsworth, Cal.) and a weighing platform to determine the evapotranspiration (ET) rate of the plants. The measured ET rate was then applied as a baseline that defined the incipient drought stress. Canopy leaf surface temperature was measured with infrared sensors (IR t/c-P, Apogee Instruments, Logan, Utah). Other environmental variables measured at the plant canopy level included dry-bulb air temperature using a type-K thermocouple, ambient air velocity using a hot-wire anemometer (TSI 8455-12, TSI, Inc., St. Paul, Minn.), light intensity using a pyranometer sensor (PY 8017, LI-COR, Lincoln, Neb.), and a relative humidity sensor (H3V-200, Rotronic Instrument Corp., Huntington, N.Y.) (Kacira et al., 2002a). These measurements were later used to determine plant CWSI. Plant top-projected images were acquired to extract leaf motion. The image acquisition system consisted of a monochrome CCD camera (Pulnix TM-200, Pulnix America, Inc., Sunnyvale, Cal.) and a 640 × 480 resolution frame grabber board (Matrox Meteor II Standard, Matrox Electronic Systems, Ltd., Dorval, Quebec, Canada) installed in a personal computer. The camera was mounted perpendicular to the horizontal plane at a height of 1.0 m above the turntable. The image seen by the camera was the top view of the plant canopy (Kacira, 2002b).

To estimate EWT of the plants from canopy multispectral reflectance, a fiber optic probe was mounted at a stationary position that was 20° from the nadir and 330 to 350 mm from the plant canopy. The fiber optic probe was connected to a spectroradiometer (PS-2, ASD, Inc., Boulder, Colo.) to collect reflectance data in the spectral range of 400 to 2500 nm. The resolution was 1 nm in the visible band and 1.5 nm in the near- and mid-infrared bands. The measurement of plant canopy reflectance was made when the plant was positioned underneath the fiber optic sensor. The reflectance measurement was taken at a 2 h interval in the

Table 1. Plant cultivars used and environmental conditions in the experiments.

		Exp 1	Exp 2	Exp 3	Exp 4	Exp 5
Plant variety		Paradise	Pure Beauty	Pure Beauty	Paradise	Paradise
Experiment duration (days)		8	8	10	16	10
Time of experiment		10-17 Nov. 2001	19-26 July 2002	7-16 Aug. 2002	23-28 Oct. 2002	20-29 Nov. 2002
Cycles of drought stress		1	1	2	2	1
Time to stop experiment		3-4 days after visual detection	2-3 days after visual detection	2-3 days after visual detection	2-3 days after visual detection	On the day of visual detection
Air temperature (°C)	Average ±SD	26.98 ±0.20	28.63 ±0.29	28.67 ±0.23	27.28 ±0.45	27.75 ±0.32
	Maximum	27.1	29.1	29.0	27.9	28.52
	Minimum	26.9	28.4	28.3	26.5	26.89
Relative humidity (%)	Average ±SD	34.6 ±1.5	53.6 ±5.6	46.8 ±3.0	27.4 ±8.4	45.9 ±8.4
	Maximum	38.4	59.3	60.8	51.3	52.4
	Minimum	33.4	44.1	33.8	18.9	38.3
VPD (Pa)	Average ±SD	2335.2 ±61.3	1851.2 ±199.6	2990.3 ±424.0	2600.6 ±348.5	2037.0 ±195.2
	Maximum	2374.0	2238.0	2576.2	3129.0	2404.9
	Minimum	2196.3	1630.6	1543.1	1783.3	1733.9
Radiation level ($J\ m^{-2}\ s^{-1}$)	Average ±SD	133. 6 ±2.6	131.2 ±4.2	133.4 ±2.3	116.7 ±1.6	114.8 ±2.2
	Maximum	135. 1	134.6	135.5	117.8	116. 9
	Minimum	132. 5	120.3	131.0	114.5	112.4
Wind velocity (m/s)	Average ±SD	0.6 ±0.1	0.6 ±0.1	0.6 ±0.1	0.7 ±0.2	0.6 ±0
	Maximum	0.8	0.7	0.8	1.2	0.8
	Minimum	0.5	0.5	0.5	0.5	0.5
Soil moisture (%)	Control average	33.5 ±4.8	57.3 ±1.7	62.4 ±1.8	74.0 ±1.9	57.9 ±2.2
	Treatment maximum	54.4	57.5	51.9	81.9	65.3
	Treatment minimum	14.3	12.2	20.3	18.9	18.1

lighting period. Each measurement was an average of 30 scans of a canopy.

Stress Indicator Extraction

ET rates were calculated using the difference between two consecutive weight measurements of the potted plants. The per unit area ET rate (kg h^{-1} m^{-2}) was calculated by taking into account the TPCA of the plant.

The CWSI values of each plant were calculated using the measured canopy temperature and environmental para‑meters. The model developed by Kacira et al. (2002b) was used in the calculation and is shown in equation 1:

$$\mathrm{CWSI} = 1 - \frac{\mathrm{ET}_a}{\mathrm{ET}_p} = \frac{\gamma\left(0.81 + \dfrac{r_s}{r_{ah}}\right) - \gamma^*}{\delta + \gamma\left(0.81 + \dfrac{r_s}{r_{ah}}\right)} \tag{1}$$

The calculation of $\mathrm{COV_{TPCA}}$ from the acquired images followed the description of Kacira et al. (2002a) and is shown in equation 2:

$$\mathrm{COV_{TPCA}} = \frac{\sigma_{\mathrm{TPCA}}}{\mu_{\mathrm{TPCA}}} \cdot 100\% \tag{2}$$

Plant canopy EWT, measured in mm of water, was used to represent plant water status. The average canopy water content of a plant was extracted from the measured reflectance spectrum using the PROSPECT+SAIL model. A reliable model inversion procedure was developed by Yang and Ling (2004) to extract EWT of New Guinea Impatiens grown under artificial lights. Inversion of the PROSPECT+ SAIL model consisted of determining simultaneously some or all of the model parameters, including chlorophyll *a* and *b* content, water content in terms of EWT, leaf internal structure index , leaf area index, and average leaf inclination angle, from measured reflectance. Because of the complexity of the model, analytical inversion of the model was prohibitive and the model was inverted numerically. The algorithm used for the inversion was the Levenberg-Marquardt algorithm (Marquardt, 1963). This algorithm was a compromise between the steepest descent method and the Gauss-Newton method, and thus combined the stability of the steepest descent method and the fast convergence speed of the Gauss-Newton method. Another advantage of this method was that it allowed user-defined search domains to define the boundaries of the dependent variables, and it did not require calculation of the second derivative of the function. By adaptively assigning leaf angle values for individual plants, searching solutions in the predefined domain, and using only mid-infrared reflectance, the procedure was able to avoid improbable local minima while searching for the best combination of plant biochemical and biophysical parameters that would produce a matching spectral curve of the measured canopy reflectance.

Threshold Value Determination

The threshold values of ET were defined using the mean values and standard deviations of the ET rates (table 2). When the ET rate of a treatment plant fell below this threshold value, the plant was identified as under drought stress.

Table 2. Definitions of threshold value of the three drought stress indicators (m and e are the mean value and standard deviation, respectively, of the indicators of non-stressed plants).

	CWSI	$\mathrm{COV_{TPCA}}$	EWT
Definition of threshold value	$\mu + 2\varepsilon$	$\mu + 2\varepsilon$	$\mu - 2\varepsilon$
Occurrence of stress when	Higher than threshold value	Higher than threshold value	Lower than threshold value

The threshold values of CWSI, COV_{TPCA}, and EWT were also determined. The definition of the threshold values for each indicator and determination of the occurrence of drought stress using each indicator are listed in table 2. Threshold values were determined by the mean plus or minus two standard deviations ($\mu \pm 2\varepsilon$) of the data points of the control plants. Using $\mu \pm 2\varepsilon$ made it possible to define the distribution of the data of the control plants at the 95% confidence interval. Data points of the treatment group that had a value within $\mu \pm 2\varepsilon$ of the control group were considered to represent well-watered plants; data points that had a value outside of $\mu \pm 2\varepsilon$ were classified as plants under water stress.

Statistical Analysis and Performance Evaluation

The SAS procedure Proc GLM (SAS for Windows, 9.01, SAS Institute, Inc., Cary, N.C.) was used in single-factor randomized ANOVA analysis on the indicator values to study if there were significant differences between the indicator threshold values in different experiments.

The performances of the indicators in drought stress detection were evaluated by comparing the timing of drought stress detection by the indicators versus the timing of ET-defined incipient drought stress, and versus the timing of visual detection. Proc GLM was adopted in separated randomized block (RBD) ANOVA analysis to examine if the timings of detection of the three indicators were statistically similar to those of incipient stress or those of visual detection. The Student-Newman-Keuls (SNK) range test was per– formed if there were significant differences.

Result and Discussion

Since data collected in different experiments showed similar trends, only the data in experiment 3 (Exp 3) are presented in the following illustration. To facilitate plant-specific discussion, a convention of Plant (plant number) is used to specify a certain plant in the experiment. For example, treatment group plant 1 in the experiment is designated as Plant(t1); control group plant 3 in the experiment is designated as Plant(c3).

ET Rates of the Plants

Difference in ET rates between control and treated plants became larger as the experiments progressed. Figure 1 shows that during Exp 3, ET rates of all plants were around 0.239 to 0.322 kg h^{-1} m^{-2} in the first two days. After day 2, ET rates of the control plants remained steady, while those of the treatment plants decreased continuously until day 5 or day 6 of the experiment, at which time the ET rates of the treatment plants were at 50% of their initial levels. On day 5 or 6, drought stress symptoms were observable on the treated plants. When drought stress symptoms were visually detected, the treated plants were irrigated again. After the re-irrigation, ET rates of the treatment plants recovered but were still lower than the initial levels.

Since the environmental conditions of the experiment were relatively stable, the threshold value of ET was defined as the mean value of daily threshold values during the experiment. Figure 1 shows that the threshold value of ET in Exp 3 was 0.206 kg h^{-1} m^{-2}. Using this baseline, incipient drought stress occurred on day 3 for both Plant(t1) and Plant(t2), and day 4 for Plant(t3).

CWSI Values of the Plants

Values of CWSI were very sensitive to changes in plant water status during the experiment (fig. 2). At the beginning of the experiment, CWSI values of the control plants were similar to those of the treated plants. As the experiment progressed, CWSI values of the treated plants increased and became larger than those of the control plants. CWSI values of the control plants remained at stable levels throughout the experiments.

In Exp 3, the threshold value of CWSI was 0.28. Using this threshold value, drought stress on Plant(t1) and Plant(t2) could be detected on day 4, which was one day after the

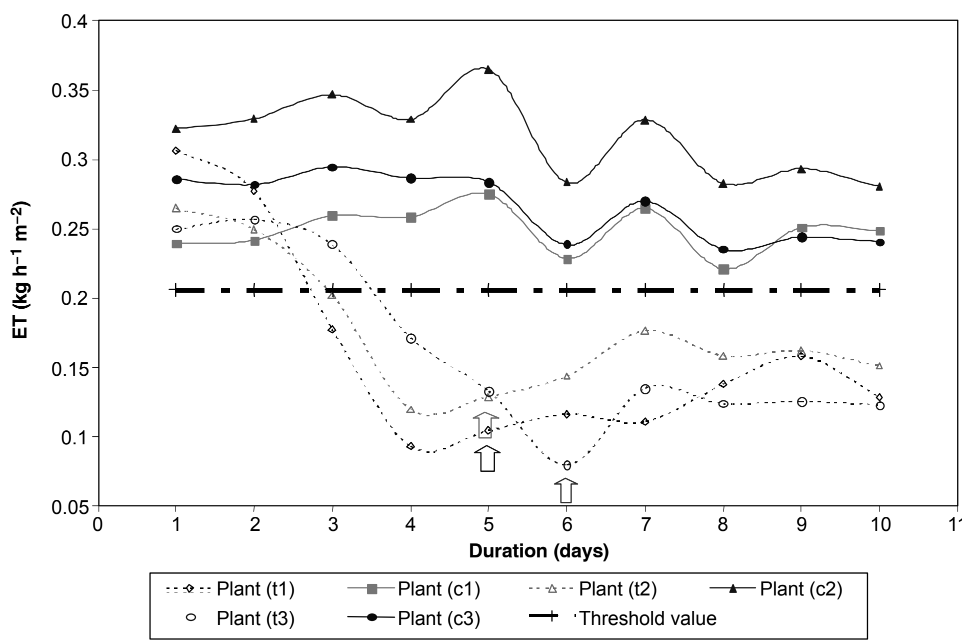

Figure 1. Daily average hourly ET rates of the plants and the ET threshold value in Exp 3. The upward arrows indicate visual detection and watering events of the treatment group plants.

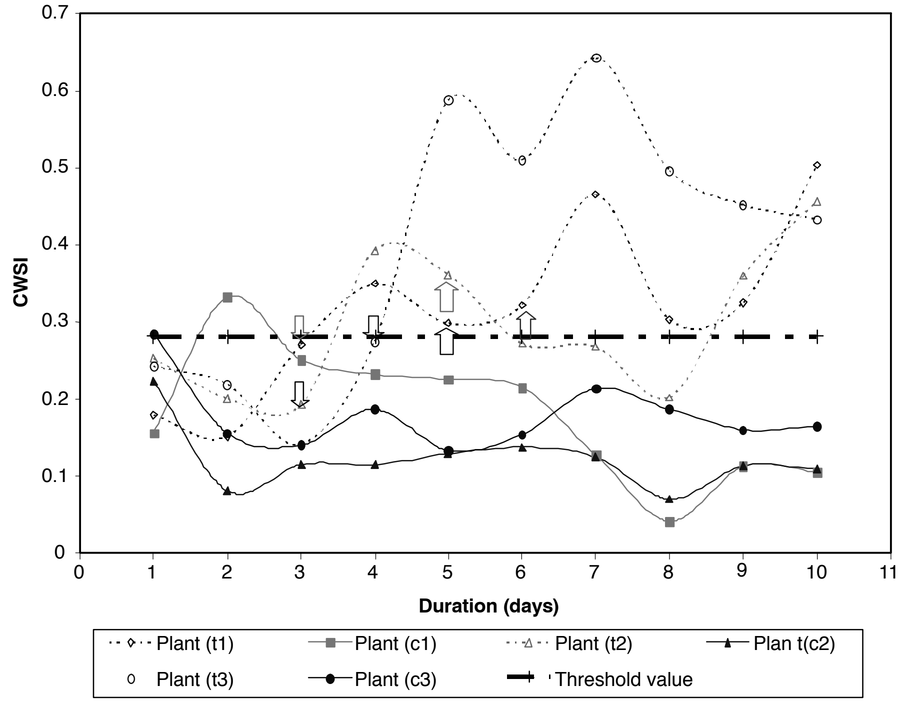

Figure 2. CWSI values of the plants in Exp 3. The upward arrows indicate visual detection and watering events of the treatment group plants. The downward arrows indicate timing of ET-defined incipient drought stress.

incipient drought stress but one day before visual detection. Drought stress on Plant(t3) could be detected on day 5, which again was one day after the incipient drought stress but one day before visual detection. CWSI values of the treatment plants decreased after re-irrigation. Values of CWSI for Plant(t1) and Plant(t2) returned to levels very close to the threshold value. Values of CWSI for Plant(t2) in fact were lower than the threshold value for three days before increasing, but the CWSI values of Plant(t3) did not decrease as much after re-irrigation. The measured ET rate showed the same trend: after re-irrigation, ET rates of Plant(t1) and Plant(t2) were higher than that of Plant(t3), and the recovered ET of Plant(t2) was the closest to the threshold value of ET.

COV_{TPCA} of the Plants

The COV of TPCA is the ratio between the daily variance in TPCA versus the daily average TPCA on the same day. In essence, it describes the magnitude of variation in TPCA

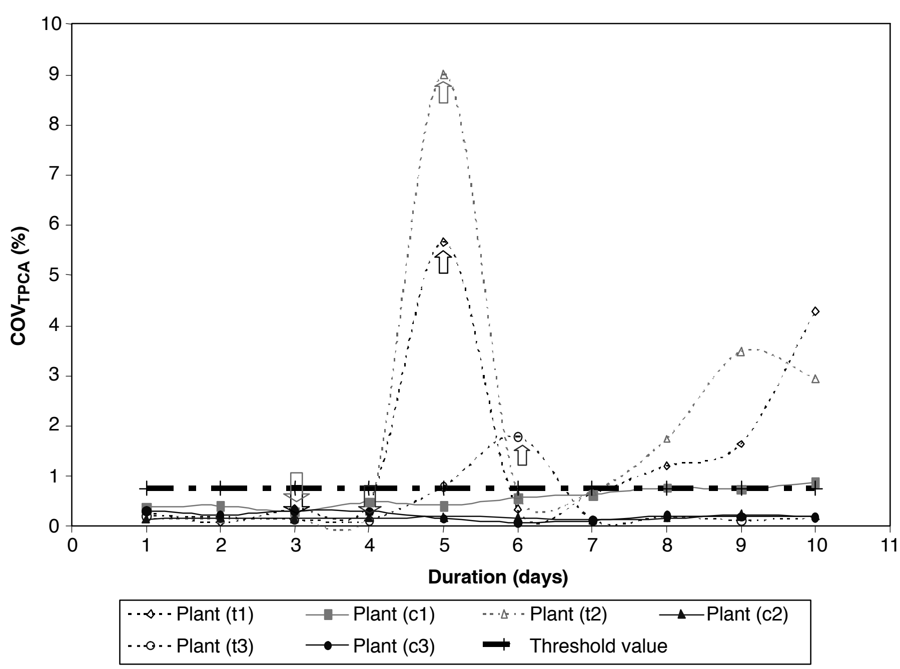

Figure 3. COV_{TPCA} of the plants and the threshold value of COV_{TPCA} in Exp 3. The upward arrows indicate visual detection and watering events of the treatment group plants. The downward arrows indicate timing of ET-defined incipient drought stress.

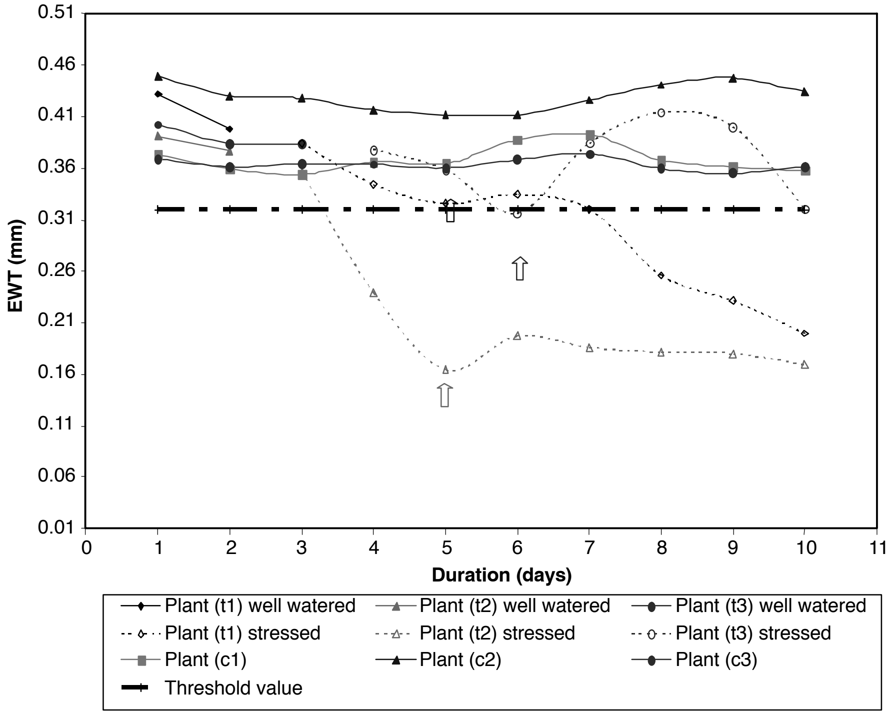

Figure 4. EWT values of the plants and the EWT threshold values in Exp 3. The solid data points represent the well-watered status defined by ET rate of the plants. The hollow data points represent the drought stressed status. The upward arrow indicates visual detection of drought stress on each treated plant.

during a certain time period (in this study, one day). As drought stress develops, the drooping of leaves occurs, causing an increase in the value of COV_{TPCA}.

Figure 3 shows that early in Exp 3, values of COV_{TPCA} of the treated plants were similar to those of the control plants. As the experiment progressed, the COV_{TPCA} values of the treated plants increased and became larger than those of the control plants. After re-irrigation, the COV_{TPCA} values for the treated plants decreased briefly. As drought stress developed again, the COV_{TPCA} values of the treated plants also increased. The COV_{TPCA} values of the control plants were stable during the experiment.

The threshold value of COV_{TPCA} in Exp 3 was 0.76%. Using this threshold value, the drought stress could be detected on day 5 of the experiment in Plant(t1) and Plant(t2), and on day 6 in Plant(t3). Figure 3 shows that threshold value of COV_{TPCA} was able to detect drought stress in the treatment plants two days after incipient drought stress, and on the same day as visual detection.

EWT of the Plants

Following the procedure determined by Yang and Ling (2004), the EWT values of the plants were retrieved from the measured spectra at an RMSE of 0.038 mm. Comparison between the EWT values of the treated plants and the control plants shows a similar trend as those of the other two indicators (fig. 4). Figure 4 shows that at the beginning of Exp 3, EWT values of the treated plants were at similar levels as those of the control plants. As the experiment progressed, EWT values of the treated plants decreased, while EWT values of the control plants remained at consistent levels.

EWT values of Plant(t1) and Plant(t2) increased slightly the day after re-irrigation, but did not exceed 0.35 mm. Afterwards, the EWT values of these plants continued to decrease until the end of the experiment. The EWT value of Plant(t3) reached its highest level at 0.41 mm three days after re-irrigation, and then decreased again. At the last day of the experiment, the EWT value of Plant(t3) was lower than 0. 35 mm.

The threshold value of EWT in Exp 3 was 0.313 mm. Using this threshold value, the drought stress of the treatment plants could be detected on days 8, 4, and 6 of the experiment for Plant(t1), Plant(t2), and Plant(t3), respectively. For the treatment plants, at all of the seven ET-defined well-watered status data points, EWT values were higher than the threshold value, while at 12 of the 23 ET-defined drought-stressed data points, the EWT values were lower than the threshold value. Figure 4 also shows that EWT was able to detect drought stress on Plant(t1) and Plant(t3) two days after incipient drought stress and on the same day as visual detection. For Plant(t2), EWT detected drought stress one day after the incipient drought stress and one day before visual detection.

Statistical Analysis Result and Performance Evaluation

ANOVA analysis of data from all experiments indicated that there were no significant differences in the values of CWSI and COV_{TPCA} of the control plants in the experiments (tables 3 and 4). However, there were significant differences in the values of EWT. Further SNK tests showed that the EWT values of control plants in Exp 2 and Exp 3 were not statistically different, but they were higher than those in the other three experiments, which were not statistically different (table 4).

The RBD ANOVA detected significant differences between timing of incipient stress defined by ET and timing of detection by the three indicators (table 5). Further SNK

Table 3. ANOVA result of the values of CWSI, COV_{TPCA}, and EWT from the control plants in the experiments.

	Source	df	SS	MS	F value	Prob.
CWSI	Model	4	0.052	0.013	2.450	0.114
	Error	10	0.053	0.005		
	Total	14	0.105			
COV_{TPCA}	Model	4	0.468	0.117	1.410	0.299
	Error	10	0.829	0.083		
	Total	14	1.297			
EWT	Model	4	0.068	0.017	44.470	<0.0001
	Error	10	0.004	0.000		
	Total	14	0.072			

Table 4. Indicator values determined from the control plants in the experiments. In each row, means followed by different letters are significantly different.

	Exp 1 Avg. of Controls	Exp 2 Avg. of Controls	Exp 3 Avg. of Controls	Exp 4 Avg. of Controls	Exp 5 Avg. of Controls
CWSI	0.18 a ±0.06	0.14 a ±0.03	0.16 a ±0.06	0.10 a ±0.03	0.08 a ±0.06
COV_{TPCA} (%)	0.48 a ±0.16	0.77 a ±0.36	0.32 a ±0.22	0.38 a ±0.11	0.23 a ±0.07
EWT (mm)	0.21 a ±0.01	0.36 b ±0.02	0.39 b ±0.04	0.25 a ±0.01	0.28 a ±0.03

tests indicated that the timing of detection by CWSI was not statistically different from the timing of incipient drought stress (table 6). Timing of detection by COV_{TPCA} and EWT was later than that of incipient drought stress, but not later than that of visual detection (table 6).

Comparing the timing of drought stress detection by indicators versus that of incipient stress and visual detection showed that CWSI was the most sensitive and most reliable indicator in drought stress detection (tables 6 and 7). Data in tables 6 and 7 show that CWSI could detect drought stress either in the same day or up to 3 days after incipient drought stress. On average, CWSI could detect plant drought stress one day after incipient drought stress occurred. This result agrees with that reported by Kacira et al. (2002a). Tables 6 and 7 also show that, on average, COV_{TPCA} could detect drought stress 2.4 days after the incipient drought stress started, while EWT was able to detect drought stress 2.3 days after drought stress started. Table 7 shows that in all the experiments, CWSI was able to detect drought stress in 87% of the treatment plants earlier than visual detection, and in 13% of the treatment plant at the same time as visual detection. COV_{TPCA} was able to detect drought stress in 33% of the treatment plants before visual detection, in 47% of treatment plants at the same time as visual detection and in 20% of the treatment plants after visual detection. EWT was able to detect drought stress in 60%, 33%, and 7% of the treatment plants, respectively, before, at the same time as, and after visual detection.

As plants experience drought stress, stomatal conductance becomes lower, reducing the transpiration rate (Grams et al., 2007). A lower transpiration rate means less latent heat is taken away from the leaf surface, and leaf temperature should increase (Liang et al., 2002; Testi et al., 2008). Canopy temperature, and therefore CWSI, is highly correlated to changes in ET. Data in table 8 show that CWSI values were highly correlated with ET in all the experiments. CWSI tracks not only the changes in canopy surface temperature but also the changes in canopy-air temperature differential. The CWSI values in this study were calculated using the modified theoretical approach (Jackson et al., 1981). As a result, CWSI values are sensitive to changes in plant water status and transpiration rate (Testi et al., 2008). This explains why the timing of detection by CWSI in the experiments was essentially the same as the timing of ET-defined incipient stress. The calculation of CWSI in essence quantifies differences in canopy surface energy balance between well-watered and drought-stressed plants. Therefore, under similar environmental conditions, the CWSI values deter–mined from the well-watered plants in different experiments should be similar. This is why there were no statistically significant differences in CWSI threshold values among the experiments.

Kacira et al. (2002a) reported CWSI threshold values of 0.20 and 0.10, respectively, in two different experiments. The threshold values in Exp 4 and Exp 5 in this study were 0.161 and 0.203, respectively, which agreed quite well with those reported by Kacira et al. (2000a). Since the ANOVA results in this study indicated that there were no significant differences in CWSI values among different experiments

Table 5. RBD ANOVA (block on experiment) results of drought stress detection timing of ET, CWSI, COV_{TPCA}, and EWT.

Source	df	SS	MS	F value	Prob.
Model	7	172.50	24.60	7.53	<0.0001
Error	52	170.10	3.30		
Total	59	342.60			

Source	df	Type III SS	MS	F value	Prob.
Method	3	45.40	15.13	4.63	0.0061
Exp.	4	127.10	31.78	9.71	<0.0001

Table 6. Average timing of drought stress detection using each of the indicators studied. Values are days after drought stress treatment started. In each column, values followed by different letters are significantly different.

	Exp 1 Mean	Exp 2 Mean	Exp 3 Mean	Exp 4 Mean	Exp 5 Mean
ET	4.7 ±0.6 a	4.0 ±1.0 a	3.3 ±0.6 a	5.0 ±1.0 a	6.0 ±0.0 a
CWSI	4.7 ±0.6 a	3.0 ±0.0 a	4.3 ±0.6 a	6.3 ±1.2 a	7.0 ±3.6 a
COV_{TPCA}	6.0 ±1.0 b	5.7 ±2.5 b	5.3 ±0.6 b	10.3 ±1.5 b	6.0 ±4.4 b
EWT	4.7 ±0.6 b	3.0 ±1.0 b	6.0 ±2.0 b	9.0 ±0.0 b	9.7 ±0.6 b
Visual	5.7 ±0.6 b	5.3 ±2.1 b	5.3 ±0.6 b	11.3 ±0.6 b	9.7 ±0.6 b

Table 7. Timing of the drought stress detection using various indicators compared against visual detection. Values are numbers of treatment plants.

	Before Visual Detection	Same Time as Visual Detection	After Visual Detection
CWSI	13	2	--
COV_{TPCA}	5	7	3
EWT	9	5	1

Table 8. Pearson correlation coefficients between CWSI and ET in the experiments. (Prob > |r| under H0: Rho = 0) is the p-value and indicates the probability of observing this correlation coefficient or one more extreme under the null hypothesis (H_0) that the correlation (Rho) is 0.

	Exp 1	Exp 2	Exp 3	Exp 4	Exp 5
Pearson's correlation coefficient between CWSI and ET	-0.92	-0.83	-0.82	-0.88	-0.74
Prob > |r| under H_0: Rho = 0	<0.0001	<0.0001	<0.0001	<0.0001	<0.0001

(tables 3 and 4), it can be concluded that the values reported by Kacira et al. (2002a) agreed quite well with the values observed in this study.

While reduced stomatal conductance results in a reduced transpiration rate, causing plant canopy temperature to increase, the reduced transpiration also helps to maintain leaf turgor pressure. Since leaf droop will not happen unless leaf turgor pressure experiences a dramatic drop, and since leaf turgor pressure does not change linearly with leaf water status, leaf droop does not develop as fast as the reduction in transpiration. This is why COV_{TPCA} was not as sensitive as CWSI in drought stress detection in the experiments.

The threshold values of COV_{TPCA} for Paradise plants were found by Kacira et al. (2002b) to be 0.70 and 0.36. The threshold values could detect the drought stress mostly at the same time of visual detection. In this study, the COV_{TPCA} threshold values of cultivar Paradise were found to be 1.02, 0.63, and 0.37, respectively, in Exp 1, Exp 4, and Exp 5. Considering that the RBD ANOVA result did not detect differences in COV_{TPCA} values of the well-watered plants in the experiments, the threshold values determined in this study agreed with previous reports quite well. Timing of the drought stress detection by COV_{TPCA} was found to be mostly one day earlier or at the same time as visual detection (tables 6 and 7).

As reduced transpiration helps to maintain leaf turgor, it also helps to reserve leaf water content. Therefore, EWT value does not decrease as quickly as transpiration rate. As the result, the threshold values of EWT in this study were not able to detect drought stress at the time of incipient stress.

In the PROSPECT model, EWT is the hypothetical thickness of a single layer of water averaged over the entire leaf. The leaf anatomy, such as leaf thickness, leaf internal structure, etc., of different cultivars is different. Consequently, the value of the parameter that is used to quantify water content in PROSPECT may also be different. In this study, plants used in Exp 2 and 3 were of the Pure Beauty variety, plants in Exp 1, 4, and 5 were of the Paradise variety. Difference in cultivar might explain why the EWT threshold values in Exp 2 and 3 were statistically similar to each other but different from those in Exp 1, 4, and 5.

From the comparison of timing of drought stress detection, it is clear that CWSI is a more sensitive indicator for plant drought stress. However, the calculation of CWSI requires many inputs, including leaf surface temperature of control plants that are well watered. In situations where well-watered control plants are not available, the CWSI model introduced in this article should not be adopted without modification. On the other hand, the data acquisition requirement for the calculation of COV_{TPCA} is relatively simpler. When an imaging instrument is available, and when the boundary between the plant canopy and the background is clear, leaf motion is still a good candidate for drought stress detection. As indicated by Yang and Ling (2004), because of the spiky characteristic of the HID light source in the near-infrared (NIR) range, the EWT values in this study were retrieved from reflectance spectra in the mid-infrared (MIR) range, which has strong water absorption features. New Guinea Impatiens is a succulent plant, which means that the leaf water content is relatively high; therefore, the absorption of light in MIR is strong. This also might explain why EWT, a direct quantitative indicator of canopy leaf water content, was not as sensitive as CWSI to the change in plant water status. However, when dealing with non-succulent plants, and if an appropriate light source is available, sensitivity of the reflectance to water content maybe enhanced, and retrieving EWT from canopy reflectance is still a method worthy of pursuing in plant drought stress detection.

Conclusions

Threshold values of CWSI, COV_{TPCA}, and EWT were established in different experiments for drought stress detection. ANOVA analysis results indicated that the threshold values of CWSI and COV_{TPCA} were stable in different experiments, while different EWT threshold values were needed for plants of different cultivar variety. The threshold values of CWSI and COV_{TPCA} established in this study agreed well with what was reported in previous studies.

ANOVA analysis of the timing of detection by the indicators showed that CWSI was the most sensitive to drought stress. The established CWSI threshold values were able to detect drought stress at the same time as incipient stress in most of the treatment plants. The performances of COV_{TPCA} and EWT were similar to each other but not as good as that of CWSI. The COV_{TPCA} threshold values detected the occurrence of drought stress in 80% of the treatment plants no later than visual detection.

The threshold values of EWT in drought stress detection were determined from measured canopy reflectance in the MIR range. These threshold values were consistent with the results found in the literature. ANOVA results indicated that EWT threshold values were not able to detect drought stress as early as CWSI threshold values, but were able to detect drought stress no later than visual detection in 60% of the treatment plants. The advantages and disadvantages of each indicator were discussed, and situations that were more appropriate for application of each indicator were discussed and recommended.

References

Aldakheel, Y. Y., and F. M. Danson. 1997. Spectral reflectance of dehydrating leaves: Measurements and modeling. *Intl. J. Remote Sensing* 18(17): 3683-3690.

Boyer, J. S. 1982. Plant productivity and environment. *Science* 218(4571): 443-448.

Bradford, K. J., and T. C. Hisao. 1982. Physiological plant ecology: II. Water relations and carbon assimilation. In *Encyclopedia of Plant Physiology*, N. S., Vol. 12B, 263-324. O. L. Lange, P. S. Nobel, C. B. Osmond, and H. Ziegler, eds. New York, N.Y.: Springer-Verlag.

Ceccato, P., S. Flasse, S. Tarantola, S. Jacquemoud, and J. Gregoire. 2001. Detecting vegetation leaf water content using reflectance in the optical domain. *Remote Sensing Environ.* 77(1): 22-33.

Ehrler, W. L., S. B. Idso, R. D. Jackson, and R. J. Reginato. 1978a. Wheat canopy temperature: Relation to plant water potential. *Agron. J.* 70(2): 251-256.

Ehrler, W. L., S. B. Idso, R. D. Jackson, and R. J. Reginato. 1978b. Diurnal changes in plant water potential and canopy temperature of wheat as affected by drought. *Agron. J.* 70(6): 999-1004.

Fereres, E., D. A. Goldhamer, and L. R. Parsons. 2003. Irrigation water management of horticultural crops. *Hortscience* 38(5): 1036-1042.

Garrot, D. J. Jr., M. W. Kilby, D. D. Fangmeier, S. H. Husman, and A. E. Ralowicz. 1993. Production, growth, and nut quality in pecans under water stress based on the crop water stress index. *J. American Soc. Hort. Sci.* 118(6): 694-698.

Garrot, D. J., Jr., M. J. Ottman, D. D. Fangmeier, and S. H. Husman. 1997. Quantifying wheat water stress with the crop water stress index to schedule irrigations. *Agron. J.* 86(1): 195-199.
Grams, T. E. E., C. Koziolek, S. Lautner, R. Matyssek, and J. Fromm. 2007. Distinct roles of electric and hydraulic signals on the reaction of leaf gas exchange upon re-irrigation in *Zea mays* L. *Plant, Cell and Environ.* 30(1): 79-84.
Goldhamer, D. A. 2005. Tree water requirements and regulated deficit irrigation. In *Pistachio Production Manual*, 103-116. 4th ed. L. Ferguson, ed. Davis, Cal.: University of California, Fruit and Nut Research and Information Center.
Halim, R. A., D. R. Buxton, M. J. Hattendorf, and R. E. Carlson. 1990. Crop water stress index and forage quality relationships in alfalfa. *Agron. J.* 82(5): 906-909.
Hsiao, J. 1981. Effects of drought stress on crop plants. In *Proc. Conf. on Biosalinity: The Problem of Salinity in Agriculture: A Conf. of Egyptian, Israeli, and American Scientists*, 72-76. Davis, Cal.: University of California.
Idso, S. B., R. D. Jackson, P. J. Pinter Jr., R. J. Reginato, and J. L. Hatfield. 1981. Normalizing the stress degree day for environmental variability. *Agric. Meteorol.* 24(1): 45-55.
Irmak, S., D. Z. Haman, and R. Bastug. 2000. Determination of crop water stress index for irrigation timing and yield estimation of corn. *Agron. J.* 92(6): 1221-1227.
Jackson, R. D., S. B. Idso, R. J. Reginato, and P. J. Pinter Jr. 1981. Canopy temperature as a crop water stress indicator. *Water Resour. Res.* 17(4): 1133-1138.
Jackson, R. D., P. J. Pinter Jr., R. J. Reginato, and S. B. Idso. 1986. Detection and evaluation of plant stresses for crop management decisions. *IEEE Tran. Geo. and Remote Sensing* GE24(1): 99-106.
Jacquemoud, S. 1993. Inversion of the PROSPECT+SAIL canopy reflectance model from AVIRIS equivalent spectra: Theoretical study. *Remote Sensing Environ.* 44(2-3): 281-292.
Jacquemoud, S., F. Baret, B. Andrieu, F. M. Danson, and K. Jaggard. 1995. Extraction of vegetation biophysical parameters by inversion of the PROSPECT+SAIL models on sugar beet canopy reflectance data: Applications to TM and AVIRIS sensors. *Remote Sensing Environ.* 52(3): 163-172.
Kacira, M., and P. P. Ling. 2001. Design and development of an automated and non-contact sensing system for continuous monitoring of plant health and growth. *Trans. ASAE* 44(4): 989-996.
Kacira, M., P. P. Ling, and T. H. Short. 2002a. Establishing crop water stress index (CWSI) threshold values for early, non-contact detection of plant water stress. *Trans. ASAE* 45(3): 775-780.
Kacira, M., P. P. Ling, and T. H. Short. 2002b. Machine vision extracted leaf movement for early detection of plant water stress. *Trans. ASAE* 45(4): 989-996.
Kanemasu, E. T., V. P. Rasmussen, and J. Bagley. 1978. Estimating water requirements for corn with a pocket calculator. Bulletin No. 615. Manhattan, Kans.: Kansas State University, Agricultural Experiment Station.
Kramer, P. J. 1969. *Plant and Soil Water Relationships*. New York, N.Y.: McGraw-Hill.
Liang, Z., F. Zhang, M. Shao, and J. Zhang. 2002. The relations of stomatal conductance, water consumption, growth rate to leaf water potential during soil drying and rewatering cycle of wheat (*Triticum aestivum*). *Botanical Studies* 43(3): 187-192.
Longenecker, D. E., and P. J. Lyerly. 1969. Moisture content of cotton leaves and petioles as related to environmental moisture stress. *Agron. J.* 61(5): 687-690.
Marquardt, D. W. 1963. An algorithm for least-squares estimation of nonlinear parameters. *J. Soc. Appl. Math.* 11(2): 431-441.
Moller, M., V. Alchanatis, Y. Cohen, M. Meron, J. Tsipris, A. Naor, V. Ostrovsky, M. Sprintsin, and S. Cohen. 2007. Use of thermal and visible imagery for estimating crop water status of irrigated grapevine. *J. Exp. Bot.* 58(4): 827-838.
Nyakwende, E., C. J. Paul, and J. G. Atherton. 1996. Plant growth assessment using edge-moment-based image analysis techniques. In *Proc. 6th Intl. Conf. on Computers in Agriculture*, 801-805. St. Joseph, Mich.: ASAE.
Naor, A. 2006. Irrigation scheduling and evaluation of tree water status in deciduous orchards. *Hort. Reviews* 32: 111-165.
Naor, A., Y. Gal, and M. Peres. 2006. The inherent variability of water stress indicators in apple, nectarine, and pear orchards, and the validity of a leaf-selection procedure for water potential measurements. *Irrig. Sci.* 24(2): 129-135.
Saini, H. S., and S. Lalonde. 1998. Injuries to reproductive development under drought stress, and their consequences for crop productivity. In *Crop Sciences: Recent Advances*, 223-248. New York, N.Y.: Food Products Press.
Samis, T. W., and D. Jernigan. 1992. Crop water stress index of ornamental plants. *Applied Eng. in Agric.* 8(2): 191-195.
Scholander, P. F., H. T. Hammel, E. D. Bradstreet, and E. A. Hemmingsen. 1965. Sap pressure in vascular plants. *Science* 148(3668): 339-346.
Testi, L., D. A. Goldhamer, F. Iniesta, and M. Salinas. 2008. Crop water stress index is a sensitive water stress indicator in pistachio trees. *Irrig. Sci.* 26(5): 395-405.
Wang, L., G. Qiu, X. Zhang, and S. Chen. 2005. Application of a new method to evaluate crop water stress index. *Irrig. Sci.* 24(1): 49-54.
Yang, Y., and P. Ling. 2001. Multi-spectral plant drought stress detection: PROSPECT model calibration. ASAE Paper No. 013074. St. Joseph, Mich.: ASAE.
Yang, Y., and P. Ling. 2004. Improved model inversion procedure for plant water status assessment under artificial lighting using PROSPECT+SAIL model. *Trans. ASAE* 47(5): 1833-1840.
Yazar, A., T. A. Howell, D. A. Dusek, and K. S. Copeland. 1999. Evaluation of crop water stress index for LEPA irrigated corn. *Irrig. Sci.* 18(4): 171-180.

Appendix

Introduction to the PROSPECT and SAIL Models

The PROSPECT model assumes that the spectral (400 to 2500 nm) properties of a leaf are a function of three variables: N, C_{ab}, and C_w (C_w is represented by EWT). A lower N value represents a compact cellular arrangement within the leaf, and a higher N value represents a more spongy cellular arrangement with more air cavities. C_{ab} and C_w affect the reflectance simulation in the visible and infrared wavebands, respectively, and they are assumed to have homogeneous distribution in a leaf. Since the model assumes that the leaf reflectance (ρ_l) and leaf transmittance (τ_l) are mainly determined by chlorophylls and water content, ρ_l and τ_l are thus independent of leaf type.

The PROSPECT model has been applied either in forward or inverse mode to simulate the reflectance of leaves with different EWT (Aldakheel and Danson, 1997) or to detect vegetation leaf water content from measured reflectance (Ceccato et al., 2001). Yang and Ling (2001) reported the relationship between EWT and RWC, which is used more often in horticulture to describe plant water status, and concluded that the EWT retrieved by inverting the PROSPECT model could be used as an indicator for water status at leaf level.

The canopy model SAIL was developed to describe the reflectance of plant canopy with different geometrical structures. This model assumes that a vegetation canopy is a homogeneous semi-infinite medium with Lambertian reflecting leaves. The azimuth angles of the leaves are

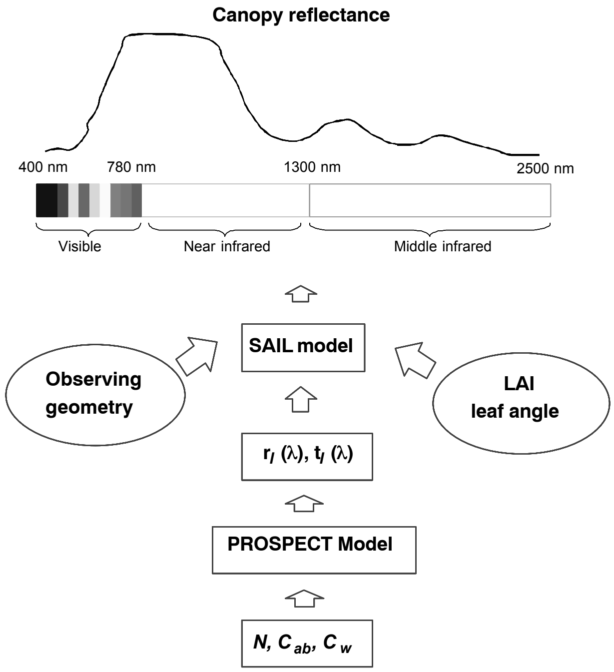

Figure A1. Diagram of the coupled PROSPECT+SAIL model. The SAIL model uses the leaf reflectance and transmittance simulated by the PROSPECT model, and the geometrical parameters, to simulate the canopy reflectance.

assumed to be randomly distributed, and the zenith angles follow an ellipsoidal distribution characterized by θ_l. LAI is used in the model to describe the plant canopy structure.

By coupling the PROSPECT and SAIL models, the PROSPECT+SAIL model computes canopy reflectance spectra (400 to 2500 nm) from the canopy parameters (C_{ab}, C_w, N, LAI, θ_l) and external parameters (zenith and azimuth viewing angles, zenith light source angle). To use the PROSPECT+SAIL model, leaf reflectance and transmittance are first simulated using the PROSPECT model, and then fed into the SAIL model. The outputs of the PROSPECT+SAIL model are, thus, functions of both canopy geometry structure and the physiological characteristics of the plant. Figure A1 shows the inputs and outputs of the models and how the models are coupled with each other.

Nomenclature

COV_{TPCA}	= covariance of top-projected canopy area (%)
C_{ab}	= chlorophyll a and b content (μg m^{-2})
C_w	= water content (mm)
CWSI	= crop water stress index
EWT	= equivalent water thickness (mm)
ET_a	= actual evapotranspiration rate (kg m^{-2} s^{-1})
ET_p	= potential evapotranspiration rate (kg m^{-2} s^{-1})
HID	= high-intensity discharge
LAI	= leaf area index
N	= leaf internal structure index
Q_{rad}	= radiation (W m^{-2})
TPCA	= top-projected canopy area (m^2)
k_H	= molecular diffusion coefficient of heat transfer in air (m^2 s^{-1})
Nu	= Nusselt number
r_{ah}	= air resistance for heat diffusion (s m^{-1})
r_s	= resistance to water vapor transfer at leaf level (s m^{-1})
RH	= relative humidity (%)
T_a	= air temperature (° C)
T_c	= canopy temperature (° C)
VPD	= vapor pressure deficit of air (Pa)
γ	= thermodynamic psychrometric constant (Pa ° C^{-1})
γ*	= thermodynamic psychrometric constant as modified by canopy aerodynamic resistance (Pa ° C^{-1})
δ	= slope of saturated vapor pressure-temperature curve (Pa ° C^{-1})
σ_{TPCA}	= variation of TPCA (m^2)
μ_{TPCA}	= mean value of TPCA (m^2)
μ	= mean value
ε	= standard deviation
ρ_l	= leaf reflectance
τ_l	= leaf transmittance
θ_l	= leaf inclination angle (°)